

Magnetic field induced chirality in Ho/Y multilayers with gradually decreasing anisotropyV. Tarnavich,^{1,*} E. Tartakovskaya,^{2,3} Yu. Chetverikov,¹ V. Golub,² D. Lott,⁴ Yu. Chernenkov,¹ A. Devishvili,⁵ V. Ukleev,^{1,6} V. Kapaklis,⁵ A. Oleshkevych,⁵ V. Fedorov,⁷ V. Bairamukov,¹ A. Vorobiev,⁵ and S. Grigoriev^{1,8}¹*National Research Center Kurchatov Institute–Petersburg Nuclear Physics Institute, 188300 Gatchina, Russia*²*Institute of Magnetism National Academy of Sciences of Ukraine, 03142 Kiev, Ukraine*³*Kiev National University, Institute of High Technologies, Glushkova ave 4-g 03022 Kiev, Ukraine*⁴*Helmholtz-Zentrum Geesthacht, 21502 Geesthacht, Germany*⁵*Uppsala University, 751 05 Uppsala, Sweden*⁶*RIKEN Center for Emergent Matter Science, 351-0198 Wako, Saitama, Japan*⁷*Saint Petersburg Academic University, 194021 St. Petersburg, Russia*⁸*Saint Petersburg State University, 198504 St. Petersburg, Russia*

(Received 1 May 2017; published 13 July 2017)

Metal rare-earth magnetic/nonmagnetic Ho/Y superlattice structures possess a coherent spin helix propagating through many superlattice layer repetitions. An external magnetic field applied in the film plane induces a nonzero average chirality of the helices. It is shown that the direction of the applied in-plane field can modify the value and sign of the chirality parameter γ . The dependence of γ on the relative angle of applied field during the field-cooling procedure has an oscillatory character and can be described by simple sinusoidal function with π periodicity. The experimental finding is discussed from the point of view of an interbalance between Zeeman energy, magnetocrystalline anisotropy, and induced uniaxial anisotropy.

DOI: [10.1103/PhysRevB.96.014415](https://doi.org/10.1103/PhysRevB.96.014415)**I. INTRODUCTION**

Heavy rare-earth (RE) elements with more than half-filled $4f$ shells exhibit several intermediate phases during the transition from the high-temperature paramagnetic to the low-temperature ferromagnetic phases. One of the intermediate magnetic phases is a so-called modulated magnetic structure, which involves an oscillatory arrangement of spins from one atomic plane to another. The modulated magnetic structure can have an oscillatory moment either in amplitude or orientation or both. The competition between the magnetic interactions in RE materials is temperature and field dependent, resulting in a complex magnetic phase diagram. The possibility to control these phases makes RE metals promising materials for magnetoelectric phenomena investigations and various nanoelectronic applications [1–3]. The magnetic ordering in these metals is associated with a long-range Ruderman-Kittel-Kasuya-Yosida (RKKY) exchange interaction between localized $4f$ electrons via conducting electrons. The most significant manifestation of the specific role of the RKKY in the formation of nontrivial magnetic structures is observed for RE superlattices (SLs) when the SL periodicity is comparable with the RKKY interaction exchange length. For instance, the spin spirals of RE metal propagate through the paramagnetic Y layer in Dy/Y or Ho/Y SL [4–6] due to an indirect exchange interaction throughout the Y layer [5].

Lately, an imbalance between the occupation number of left- and right-handed spirals was discovered in helimagnetic Dy/Y that occurs when the sample was cooled down to helimagnetic phase [7] without any additional treatment as, e.g., the application of a magnetic field during the cooling procedure. This finding was surprising since the RKKY interaction responsible for the formation of the helical phase

is an even function of the propagation vector and cannot be the cause for the occurrence of a difference in the occupation numbers of left- and right-handed spirals in Dy/Y. Additional measurements of the structural composition of the Dy/Y sample revealed that the crystallographic c axes and the interfaces of Dy/Y SLs have a considerable mismatch and thus indicated that the Dzyaloshinskii-Moriya interaction (DMI) may be responsible for the chiral behavior in this sample [7].

The influence of DMI on the chirality was already shown earlier in stacked triangular antiferromagnets when they are cooled in electric fields [8] or, lately, in magnetic systems underlying curvature and torsion [9,10]. In the latter case, equilibrium magnetization states in magnetic helix nanowires with different anisotropy axis show that curvature and torsion have influence on the spin-wave dynamics, acting as an effective magnetic field, originated from a geometry induced DMI. This magnetic field leads to a coupling between the helix chirality and the magnetochirality and breaks mirror symmetry in the spin-wave spectrum.

For the Dy/Y SL, the presence of a nonzero DMI contribution was subsequently confirmed by theoretical calculations showing that a macroscopic DMI will form considering the tilted configuration between the crystallographic configuration and the interfaces [11]. Moreover, inelastic neutron measurements on the same Dy/Y SL sample, revealing for the first time the presence of discrete energy levels in the SL systems, also confirmed the need of an additional energy term in the form of the DMI to describe the quantitative behavior of the observed inelastic energy spectra [12].

Beside the chirality effect at zero field cooling (ZFC), it was also found that the chirality can be influenced by the application of an in-plane magnetic field during the cooling procedure [field cooling (FC)], and its value depends mainly on the strength of the magnetic field applied during the FC procedure [7]. For several Dy/Y samples and Ho/Y samples with only very little mismatch between the crystallographic c

*tarnavich_vv@npni.nrcki.ru

axes and the interfaces that showed, as expected, no imbalance of left- and right-handed spirals during the ZFC procedure, a similarly sized chirality effect could be introduced and manipulated by the application of an in-plane magnetic field applied during the FC procedure [13,14]. Model calculations taking into account the RKKY and Zeeman energy could reveal that here an additional energy term is needed that introduces a difference in the energy levels between left- and right-handed spirals. A DMI term was considered to be the most likely candidate as it was already found for the ZFC case of the sample with the slightly tilted interfaces.

Contrary to the ZFC case, however, no direct mechanism could be exemplified for the FC introduced chirality effect. The opposite sign of the chirality effect in the ZFC case in respect to the FC case is suspected to be caused by the interplay between the Zeeman, RKKY, and DM interactions, and consequently the sign may not be directly linked with the orientation of the DM vector [13]. Lately, when a series of Ho/Y multilayers with different layer compositions was investigated, it turned out that no or only very small chirality effect could be introduced for some of the Ho/Y SLs during the FC procedure [15]. No relation of the bilayer or sample compositions, e.g., due to sample quality or the thickness relation between the Ho and Y layer that may cause a destructive interference effect, could be found to be responsible for the absence of the expected chirality effect. It raised the question whether alternative mechanisms play a role in the activation of chirality in these multilayer structures, e.g., that the chirality parameter may also depend on the relative orientation of the in-plane field and the ab plane of the SL. Originally such a dependence was not considered due to the absence of any appreciable magnetic anisotropy in the ab plane of Ho [16] as well as in Dy [17]. Consequently, it was assumed that there is no relation between the field orientation in the ab plane, and due to the antisymmetric DMI, no influence of the in-plane magnetic field direction on the sample chirality is expected.

In the present paper, we introduce an alternative concept that may be responsible for the occurrence of chirality in such helical SL structures during the FC procedure without the need of the assumption of an interfacial DMI. It is based on the presence of an anisotropy term that is nonhomogeneously distributed along the z direction as, e.g., it could be caused by the presence of interfaces or introduced by structural defect of the substrate. Such gradient anisotropy formation in layered structures was investigated in Ref. [18]. The theoretical model will be supported by experimental results on a Ho/Y SL, which are presented in the following. It provides the opportunity to identify such phenomena of magnetism that are sensitive to effects that may occur due to particular preparation techniques as, e.g., the choice of the supporting substrate and its structuring.

A. Model calculations: chirality effect in Ho/Y SL due to anisotropy

Let us consider an alternative mechanism of the chirality switching in such multilayer systems. It is well known that the magnetic helical order is established due to the RKKY interaction [19,20]. The energy of the RKKY interaction is

an even function of the pitch angle of the helix, and it does not depend on the sign of helical vector component k . As a result, the RKKY interaction cannot lead to a nonzero chirality in the helical structure itself. On the other hand, such a nonzero net chirality can be established due to the interplay of RKKY, Zeeman, and DM interactions [13,21]; however, in the following we will demonstrate how chirality effects can occur in such helical SL systems without the need of introducing the asymmetric DMI interaction.

The magnetic helical order, established in the sample, is considered as a simple spiral, where the spins lay in the plain of the film, perpendicularly to the helical vector \mathbf{k} . The helical vector $\mathbf{k} = (0, 0, k)$ is parallel to the film normal (z axis). Then xy plane is lying in the film plane, and vector \mathbf{k} is perpendicular to it. The sign of the z component of the \mathbf{k} vector, k , defines the domain's chirality by being positive or negative.

It is valid to assume that the RKKY exchange is the strongest interaction in the system and that the length of the helical vector does not change significantly under the application of a moderate external magnetic field or a magnetocrystalline anisotropy field with its anisotropy easy axis lying in the film plane. The external magnetic field as it is applied during the FC procedure is along the x axis, even though the x axis lies in the film plane arbitrarily. $|\mathbf{H}| = H_x = H$ and the angle between \mathbf{H} and the anisotropy axis are denoted as ψ .

The angle φ_0 is defined as the angle between the spin in the middle of the magnetic layer and the applied magnetic field. The Zeeman energy of the layer of the thickness d can be now written as [13],

$$\begin{aligned} W_Z(\varphi_0, k) &= -HM_0 \int_{-d/2}^{d/2} \cos(\varphi_0 + k \cdot z) dz \\ &= \frac{-2HM_0d}{kd} \cos(\varphi_0) \sin(kd/2), \end{aligned} \quad (1)$$

where M_0 is the staggered magnetization of the magnetic atomic layer. $W_Z(\varphi_0, k)$ reaches its minimum at $\varphi_0 = 0$ if $\sin(kd/2) > 0$ (i.e., $kd < 2\pi$) and at $\varphi_0 = \pi$ if $\sin(kd/2) < 0$ ($2\pi < kd$). This corresponds to the situation in which the resulting vector of the magnetization of the layer is always directed along the applied field in the absence of any competing anisotropy.

In the next step we assume that a nonhomogeneous anisotropy is present in the system that, e.g., may have its origin from the fabrication process. The energy of the uniaxial magnetocrystalline anisotropy in a collinear ferromagnet usually is written in the form $M_0^2 A \cos^2(\zeta)$, where ζ is the angle between the magnetization and the easy axis. In the case of the noncollinear helical structure of the RE SLs discussed here, the formula results in

$$\begin{aligned} W_A(\varphi_0, k, \psi) &= -M_0^2 A \int_{-d/2}^{d/2} f(z/d) \\ &\quad \cdot \cos^2(\psi - (\varphi_0 + k \cdot z)) dz, \end{aligned} \quad (2)$$

where A is a dimensionless constant of the uniaxial anisotropy with $A > 0$. We assume that the anisotropy effect is maximally on one of the faces of the system and that the anisotropy is not homogeneous along the z direction but here assumed

to decrease with increasing distance from the substrate. That scenario is accounted for with the function $0 < f(z/d) < 1$, which monotonically decreases while z is increasing.

When the direction of the magnetic field is parallel to the anisotropy axis, i.e., $\psi = 0$ or $\psi = \pi$, the angle φ_{\min} , which minimizes the energy functional $W(\varphi_0, k, \psi) = W_Z(\varphi_0, k) + W_A(\varphi_0, k, \psi)$, is also equal to 0 or π and thus follows the scenario as it is described above for the Zeeman energy. If the angle between \mathbf{H} and the anisotropy axis is not parallel, i.e., $\psi \neq 0, \pm\pi$, the angle φ_{\min} that minimizes the energy functional is determined by the competition between the anisotropy and Zeeman energies.

In order to investigate whether the energy functional, which is the sum of the Zeeman and the anisotropy energies, depends on the sign of k and thus on the handedness, $W(\varphi_0, k, \psi)$ was numerically calculated by using formulae (1) and (2) for a series of values of ψ and kd . In Fig. 1, the results for three selected values of angles between the anisotropy axis and the applied magnetic field direction are shown for both handedness with values of $kd = \pm 2\pi/3$. The numerical calculations unambiguously demonstrate that the energies of the chiral domains with opposite signs of the helical vector are different in these cases, which lead to the energetically preference for domains with a definite handedness [see insets to Figs. 1(a), 1(b), and 1(c)].

With a value $|kd| < 2\pi$ and the anisotropy energy much smaller than the Zeeman energy (see text below), the angle φ_{\min} for which $W(\varphi_0, k, \psi)$ reaches its minimum, is close to zero. For $|kd| > 2\pi$, the corresponding φ_{\min} is close to π (not shown here); however, the main conclusion about the difference in the domain's energies for the two handedness persists. In all figures and their insets, the black and red solid lines present calculations for the value $kd = 2\pi/3$ and $kd = -2\pi/3$, respectively. Comparing the insets of Figs. 1(a) and 1(b) leads to the conclusion that the difference between the values of the energies of chiral domains with $kd = 2\pi/3$ and $kd = -2\pi/3$ is larger for the case of $\psi = \pi/4$ than for $\psi = \pi/6$. For $\psi = \pi/2$, the difference becomes zero (not shown), and, consequently, the chiral parameter changes its sign for larger angles, as shown in Fig. 1(c), where the black and red lines have “changed position” for $\psi = 3\pi/4 > \pi/2$. Obviously, a coupling between the symmetry of the anisotropy and the symmetry of the chirality exists. At first, it is essential to identify how such a system behaves without the assumption of certain kd and ψ values. The minimum of the general energy functional $W(\varphi_0, k, \psi) = W_Z(\varphi_0, k) + W_A(\varphi_0, k, \psi)$ has to be calculated with

$$\left. \frac{\partial W(\varphi_0, k, \psi)}{\partial \varphi_0} \right|_{\varphi_0 = \varphi_{\min}} = 0.$$

Here, φ_{\min} satisfies the relation

$$2H \sin(\varphi_{\min}) \sin\left(\frac{kd}{2}\right) - M_0 kd A \int_{-d/2}^{d/2} f(z/d) \cdot \sin(2\psi - 2(\varphi_{\min} + k \cdot z)) dz = 0. \quad (3)$$

This integral equation does not have an exact analytical solution but can be very well approximated by the well-developed method of perturbation theory. Previous investigations of an induced anisotropy [22] showed that the anisotropy

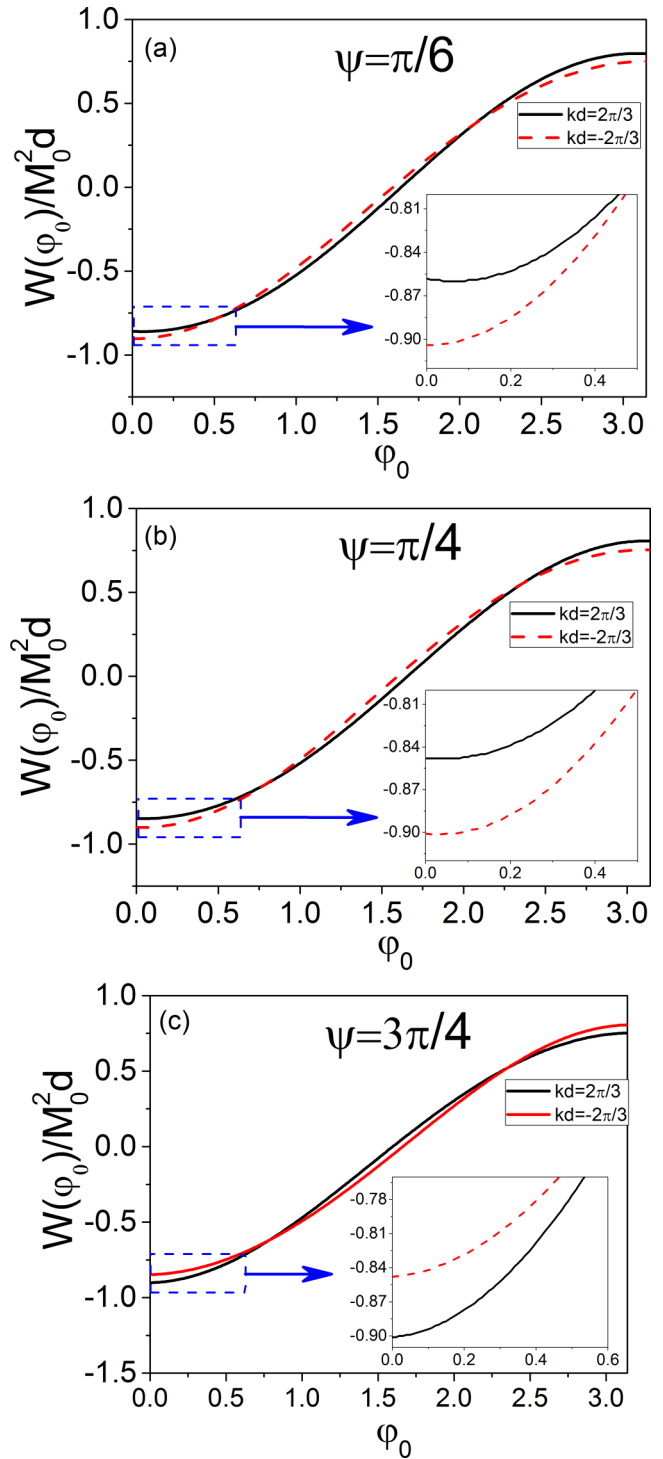


FIG. 1. Energy functional $W(\varphi_0, k, \psi) = W_Z(\varphi_0, k) + W_A(\varphi_0, k, \psi)$ with $\frac{AM_0}{H} = 0.15$, calculated as a function of the angle $0 < \varphi_0 < \pi$ for values $|kd| = 2\pi/3$ and different values of ψ , as noted in the figures. The function $f(z/d)$ in formula (2) was chosen as $f(x) = \exp(-3(x + 1/2))$. Insets: Enlargements of the main figures, taken for smaller area of φ_0 in the vicinity of the energies' minima.

field can be estimated to be about tens of an Oersted and thus is at least one order less than the applied field in our experiments (see below). It is therefore reasonable to assume that the value of an induced magnetic anisotropy field is much smaller than

the external magnetic field, i.e., $\frac{AM_0}{H} \ll 1$. Then, according to (3),

$$\sin(\varphi_{\min}) \approx \frac{M_0 A k d}{2H \sin(kd/2)} \int_{-d/2}^{d/2} f(z/d) \cdot \sin(2\psi - 2k \cdot z) dz. \quad (4)$$

Expression (4) shows that the value of $\sin(\varphi_{\min})$ is small and of the same order as the parameter $\frac{AM_0}{H} \ll 1$, thus it follows

$$|\sin(\varphi_{\min})| \propto \frac{AM_0}{H} \ll 1$$

$$|\cos(\varphi_{\min})| \approx 1.$$

In a first approximation the anisotropy energy (2) can now be written as

$$W_A(\varphi_{\min}, k, \psi) = -\frac{M_0^2 A}{2} \int_{-d/2}^{d/2} f(z/d) dz$$

$$- \frac{M_0^2 A}{2} \int_{-d/2}^{d/2} f(z/d) \cos(2\psi - 2k \cdot z) dz. \quad (5)$$

In the following, we analyze the dependence of the obtained expression $W(\varphi_{\min}, k, \psi)$ on the sign of the propagation vector k . The difference of the energies of the domains with different handedness results subsequently from (5) to

$$\delta W_{\text{chiral}} = W_A(\varphi_{\min}, k, \psi) - W_A(\varphi_{\min}, -k, \psi)$$

$$= -2M_0^2 A \sin(2\psi) \int_{-d/2}^{d/2} f(z/d) \cos(k \cdot z) \sin(k \cdot z) dz.$$

It should be noted that the obtained expression can be also written in a form that is similar to the DMI interaction (pseudo-DMI):

$$\delta W_{\text{chiral}} = -2A \sin(2\psi) \int_{-d/2}^{d/2} f(z/d) \cos(kz) [\mathbf{M}_i \times \mathbf{M}_{i+1}]_z dz,$$

with $[\mathbf{M}_i \times \mathbf{M}_{i+1}] = (0, 0, M_0^2 \sin(kz))$.

The corresponding chiral parameter can finally expressed as

$$\gamma = \frac{I^+ - I^-}{I^+ + I^-} \propto \delta W_{\text{chiral}}$$

$$= -M_0^2 A \sin(2\psi) \int_{-d/2}^{d/2} f(z/d) \sin(2k \cdot z) dz. \quad (6)$$

A straightforward analysis of relation (6) leads to the following conclusions:

(1) $\gamma \propto \sin(2\psi)$, i.e., γ is equal to zero when $\psi = 0, \pm \pi/2, \pi$.

(2) If $f(z) = \text{const}$, then γ is equal to zero.

It should be noted that corresponding calculations demonstrate that in case of an induced anisotropy of an n -symmetry – described by the formula $M_0^2 A \cos^4(\zeta)$ in a collinear ferromagnet and, correspondingly, by the formula $W_A(\varphi_0, k, \psi) = -M_0^2 A \int_{-d/2}^{d/2} f(z/d) \cdot \cos^4(\psi - (\varphi_0 + k \cdot z)) dz$ – the chiral parameter of the resulting induced chirality has a dependence of $\sin(n\psi)$. Therefore, the symmetry of the anisotropy is transferred into the chirality parameter, i.e., twofold symmetry corresponds to a $\sin(2\psi)$ or a fourfold symmetry corresponds to a $\sin(4\psi)$ dependency.

Summarizing the results of the model calculation, a spatially inhomogeneous anisotropy distribution along the sample normal may result in an additional chirality of the here observed symmetry. In other words, if some anisotropy is imprinted in the system that is not homogeneously distributed along the sample normal as, e.g., due to interfacial defects or originating from the substrate and the growth process, then such helical multilayers have the potential to show chirality effects during the FC procedure. The calculations also demonstrate that in this case the relative angle ψ between the applied in-plane magnetic field and the anisotropy axis will define the size of chirality effect and show a sinusoidal dependence on the azimuthal angle. If the chirality effect during the FC procedure would be due to only an interfacial DMI in combination with the Zeeman and RKKY interaction, as assumed in Refs. [7] and [13], no dependence of the chirality parameter on the azimuthal angle ψ should be observed. In the following chapter, the experimental results on the chirality effect on a Ho/Y SL will be described where the dependence of its chirality on the azimuthal angle is investigated.

II. EXPERIMENT

The Ho/Y SL samples consisting of 30 periods of $[\text{Ho}_{45\text{\AA}}/\text{Y}_{30\text{\AA}}]$ and $[\text{Ho}_{60\text{\AA}}/\text{Y}_{30\text{\AA}}]$, denoted as (Ho45Y30) and (Ho60Y30), were deposited on sapphire substrates with a Nb buffer layer via molecular beam epitaxy. The sample preparation details can be found elsewhere [14]. The crystal structure was determined using a standard x-ray tube diffractometer ($\text{CuK}\alpha_1$ radiation) in the wide angle diffraction and reflectometry modes. The x-ray diffraction has shown the formation of an epitaxial Ho/Y SL film with the hexagonal [001] c axis perpendicular to the film plane. The structural coherence length of the SL is of about 500 Å, and the average mosaicity is of about 0.34° (see Refs. [14] and [15] for details).

The polarized neutron diffraction technique was used to determine the magnetic chirality [7,13,14]. The experiments were carried out on the Super-ADAM polarized neutron reflectometer (Institut Laue-Langevin, Grenoble, France) using incident neutron beam with a polarization $P = 99.7\%$ at a wavelength $\lambda = 5.183$ Å with $\Delta\lambda/\lambda = 0.035$. To determine the chirality parameter γ , the polarization-dependent asymmetric part of the magnetic neutron-scattering cross section was measured [7,13,14]:

$$\gamma = \left| \frac{1}{P_0} \frac{I(+P_0, \mathbf{Q}) - I(-P_0, \mathbf{Q})}{I(+P_0, \mathbf{Q}) + I(-P_0, \mathbf{Q})} \right|, \quad (1)$$

where $I(+P_0, \mathbf{Q})$ and $I(-P_0, \mathbf{Q})$ are the intensities of scattered neutrons at the definite point in the reciprocal space $\mathbf{Q} = \mathbf{k}$ and with the polarizations parallel (+) or antiparallel (–) to the initial polarization P_0 , they originate from the incommensurate helical spin structure. The value of the chirality parameter γ is proportional to the difference between the number of left- and right-handed spin spirals, or, in the present case, the volumes of left- and right-handed domains: $|\gamma| = 0$ corresponds to an equal concentration of left- and right-handed domains as $|\gamma| \neq 0$ corresponds to a prevalence of domains of one type and thus the presence of a chiral state. The experimental geometry used to determine the polarization-dependent part of the scattering cross section and

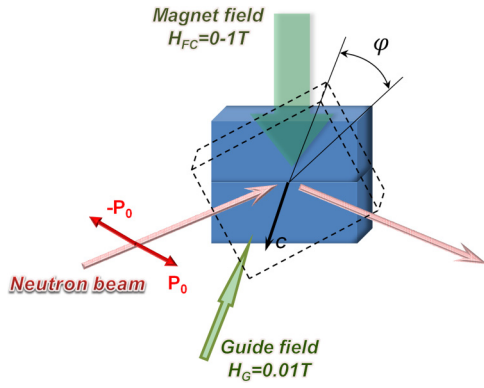


FIG. 2. The scheme of the experimental geometry.

to distinguish chiral contribution is shown in Fig. 2. The c axis of the multilayer sample was orientated perpendicular to the direction of the incident beam. The magnetic field H_{FC} up to 10 kOe was applied parallel to the multilayer surface during the FC procedure from $T > T_N$ to $T < T_N$, where T_N is the Néel temperature of Ho. To distinguish the chiral contribution, a small guide field $H_G \approx 10$ Oe was applied parallel to the c axis with $\mathbf{H}_G \parallel \mathbf{P}_0 \parallel \mathbf{k}$ while the polarization direction of the incident neutron beam could be adiabatically rotated transversely to the sample plane after the FC procedure the in-plane field H_{FC} was switched off. After each measurement, the sample was rotated in the film plane within $\sim \pi$.

III. RESULTS

The chirality measurements were performed after both FC and ZFC procedures. Within the experimental error, no difference was observed in the chirality-dependent scattering intensities after the ZFC procedure in the previous works [14,15] either in the present experiment. However, a clear difference between the scattering intensities for the two opposite polarizations appears after the FC procedure. Figure 3

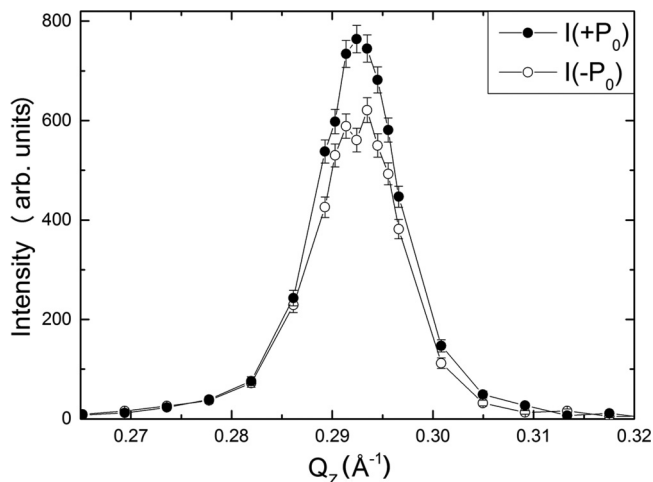


FIG. 3. The wave vector transfer Q_z dependence of the neutron scattering intensity (reflectivity profile) for the sample Ho45Y30 obtained for two polarizations of the incident beam at $T = 60$ K after FC procedure in the applied field $H_{FC} = 8$ kOe.

shows reflectivity profiles, $I(+P_0)$ and $I(-P_0)$, for the sample Ho45Y30 cooled down to 60 K in a magnetic field of $H_{FC} = 8$ kOe. The Bragg peak arises from the magnetic ordering below Néel temperature ($T_N = 118$ K) and corresponds to the incommensurate basal-plane helix magnetic structure.

The nonzero difference of the two scattering intensities for two opposite polarizations $I(+P_0)$ and $I(-P_0)$ is the result of an unequal population of domains with opposite spin chirality. It has been shown that γ depends on the applied magnetic field H_{FC} and is practically independent of the cooling temperature [14].

In a subsequent step, we investigated the dependence of the value of γ on the direction of the applied magnetic field in the sample plane applied during the FC procedure. Figure 4 shows the result for a range in the azimuthal angle ψ^* of approximately π . It clearly demonstrates that the value of γ depends in an oscillatory way on the direction of applied magnetic field in both the value and the sign. The chirality parameter can be described very well by a simple sine function with a periodicity of about $2\psi^*$ of the azimuthal angle and an amplitude of $\gamma = 0.12$.

For the sample Ho60Y30 [Fig. 4(a)], only a very small chirality effect was introduced during the FC procedure if mounted in the rectangular configuration, as has been reported earlier [15]. However, the present paper reveals that the azimuthal dependence of γ parameter for the Ho60Y30 sample, as shown in Fig. 4(b), is quasi-identical for Ho45Y30 under considering the error bars due to the manual alignment procedure. It also exhibits a dependency of the γ parameter of a periodicity of about π , with the difference that the γ parameter is significantly smaller compared to the sample Ho45Y30 with a maximum of only about 0.04. The quasi-identical dependence of the chirality parameter on the azimuthal angle for both samples supports the assumption of the general nature of the researched phenomenon.

It should be noted that a direct interaction between the spin chirality and the applied magnetic field breaks the time-reversal symmetry and is therefore forbidden. Recent investigations of the phase transition in a chiral helimagnet prove this point [22]. Here, it has been demonstrated that one may get a chiral magnetic soliton lattice under the application of a magnetic field, but the initial spin chirality cannot be changed. This finding clearly demonstrates that the dependence of the chirality effect on the relative angle of the in-plane cooling field found here indicates strongly that a nonhomogeneous twofold anisotropy is present in the system that let apply the above discussed mechanism for the occurrence of the chirality effect in the system.

In the search for the source of such an inhomogeneous anisotropy of the sample, atomic force microscopy (AFM) measurements were carried out using an Omicron UHV AFM/STM instrument (Uppsala University, Sweden), operated in the contact AFM mode. In the Fig. 5, one can clearly see ordered terraces with a mean distance between the terraces of about $0.5 \mu\text{m}$.

The appearances of such terraces can be linked to the applied polishing procedure of sapphire substrates before the growth of the SL samples. The mechanisms of an appearance of the uniaxial anisotropy on substrates with terraces were discussed in Refs. [23] and [24]. It should be noted that

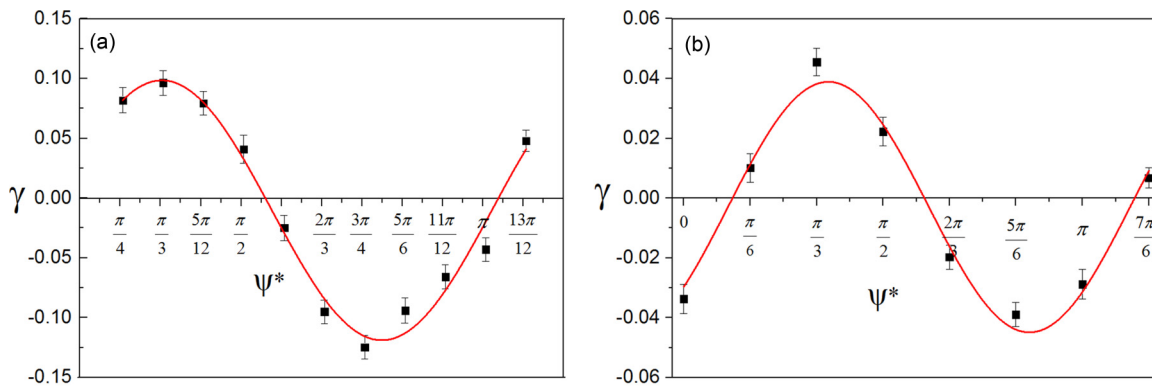


FIG. 4. Azimuthal dependence of γ parameter for the samples Ho45Y30 (a) and Ho60Y30 (b) after FC procedure to 60 K in the field $H_{FC} = 8$ kOe. ψ^* denotes the azimuthal angle with the zero position aligned by eye of the experimentalists at the rectangular position, i.e., when the edges of the sample are parallel to the neutron beam direction.

such anisotropy is related to the substrate/film interface and therefore may gradually decrease with the distance from the substrate.

Figure 6 shows a map of the crystallographic axes of the multilayer structure for the sample Ho45Y30, the terraces of the substrate, and its chirality switching.

Since the magnetocrystalline anisotropy in the ab plane of holmium is negligibly small and far off the zero γ direction, it can be excluded as a potential candidate for explaining the observed chirality effect. The direction of terraces of the substrates, on the other hand, coincides well with one of the zero γ direction within the errors bars due to the manual alignment procedure that can be estimated by $\Delta\psi = \pm\pi/36(5^\circ)$. The value of the angle was obtained from a comparison of sample orientation and the direction of terraces on purified substrate. Therefore, it may explain well the origin of the anisotropy axis present in the sample as well as the required inhomogeneity of the anisotropy along the z

direction since it will be strongest at the interface between the SL structure and the substrate. When the temperature is decreased, RKKY becomes stronger, and the formation of the helices starts; however, now the imprinted anisotropy plays an important role with its relative direction in respect to the applied field. The anisotropy forces the moments along its direction, and thus, if the angle is closer for a left or right turn it should create more of one of the handed directions of the spirals. Consequently, we observe chirality. In the case of Ho/Y, this scenario is already reached in close vicinity of the helical transition temperature.

It should be pointed out that the hypothesis presented here does not negate the presence of an interfacial DMI in this system. Obviously, the induced effective uniaxial magnetic

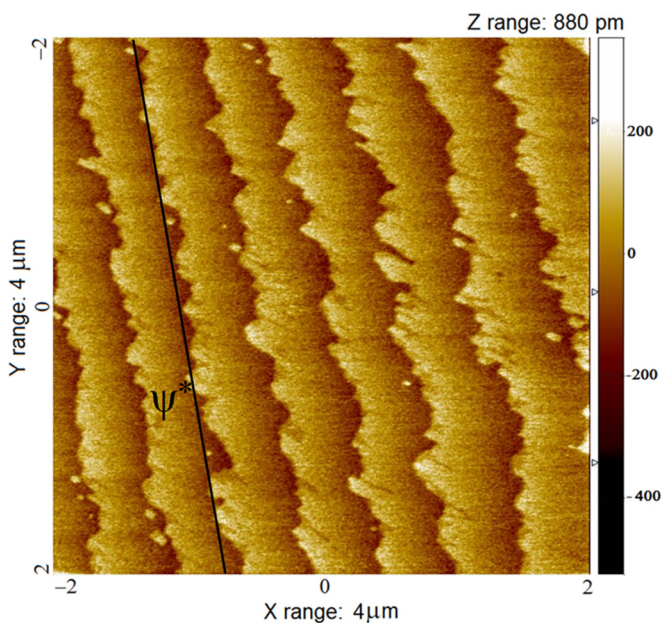


FIG. 5. Representative AFM image of the polished sapphire (11–20) substrate before the SL deposition.

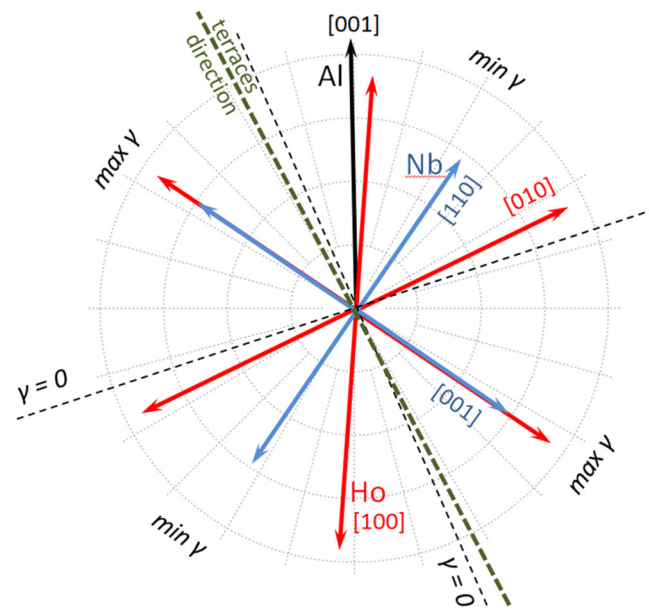


FIG. 6. A map of the crystallographic axis of the multilayer structure for the sample Ho45Y30 and its chirality switching. The directions of crystallographic axes are shown as red lines for Ho (coinciding with Y axes), blue lines for buffer and cup Nb layers, and black lines for sapphire (Al). The dotted lines correspond to the direction of the magnetic field when the γ value is equal to zero. The green line is the direction of terraces on sapphire substrate.

anisotropy may coexist with the DMI. Therefore, the nonzero net chirality is a direct result of imperfections of the forming magnetic structure by cooling it throughout the transition temperature.

The effect of the substrate relief is one of the possible and, here, most likely scenarios, leading to the observed chirality effect and its azimuthal dependence. At the same time, an appearance of the induced uniaxial anisotropy can be related to deviation of growth plane from the base crystallographic plane or a misfit of crystallographic axis of Nb and Y(Ho). In all cases, the influence of structural defects in the formation of the magnetic state is obvious, as described above.

IV. CONCLUSION

Based on the experimental observation by polarized neutron diffraction technique, we can draw the conclusion that the overall chirality balance depends on the relative orientation of the *ab* plane of the Ho/Y SL and the applied magnetic field during the FC procedure. The dependence of an oscillatory

character can be described by a simple sinusoidal function with π periodicity and explains the absence of chirality in certain previous experiments [15]. We found strong indication that the presence of substrate terraces is responsible for an induced effective uniaxial magnetic anisotropy, inhomogeneously distributed along the *z* direction, that favors a certain handedness of the spin spirals. This finding opens a new way for manipulating the handedness of such systems by introducing an artificially induced anisotropy that would be impossible if only the DMI would be the cause of chirality effects.

ACKNOWLEDGMENTS

The present work is carried out with the financial support of the Ministry of Education and Science of the Russian Federation, the Agreement on provision of Grant No. 14.616.21.0004, unique identifier of agreement RFMEFI61614X0004. E. Tartakovskaya and V. Golub appreciate the financial support of the nanoscience and nanotechnology Grant No. 1/17-H provided through National Academy of Sciences of Ukraine.

-
- [1] A. K. Zvezdin and A. A. Mukhin, *JETP Lett.* **88**, 505 (2008).
- [2] Y. Tokunaga, Y. Taguchi, T. Arima, and Y. Tokura, *Nat. Phys.* **8**, 838 (2012).
- [3] S. Bertaina, S. Gambarelli, A. Tkachuk, I. Kurkin, B. Malkin, A. Stepanov, and B. Barbara, *Nat. Nanotechnol.* **2**, 39 (2007).
- [4] S. V. Grigoriev, Yu. O. Chetverikov, A. I. Okorokov, D. Yu. Chernyshev, H. Eckerlebe, K. Pranzas, and A. Schreyer, *JETP Lett.* **83**, 478 (2006).
- [5] D. A. Jehan, D. F. McMorrow, R. A. Cowley, R. C. C. Ward, M. R. Wells, N. Hagmann, and K. N. Clausen, *Phys. Rev. B* **48**, 5594 (1993).
- [6] R. W. Erwin, J. J. Rhyne, M. B. Salamon, J. Borchers, S. Sinha, R. Du, J. E. Cunningham, and C. P. Flynn, *Phys. Rev. B* **35**, 6808 (1987).
- [7] S. V. Grigoriev, Yu. O. Chetverikov, D. Lott, and A. Schreyer, *Phys. Rev. Lett.* **100**, 197203 (2008).
- [8] M. L. Plumer, H. Kawamura, and A. Caillé, *Phys. Rev. B* **43**, 13786(R) (1991).
- [9] K. V. Yershov, V. P. Kravchuk, D. D. Sheka, and Y. Gaidi Dei, *Phys. Rev. B* **92**, 104412 (2015).
- [10] K. V. Yershov, V. P. Kravchuk, D. D. Sheka, and Y. Gaidi Dei, *Phys. Rev. B* **93**, 094418 (2016).
- [11] J. T. Haraldsen and R. S. Fishman, *Phys. Rev. B* **81**, 020404(R) (2010).
- [12] A. T. D. Grünwald, A. R. Wildes, W. Schmidt, E. V. Tartakovskaya, J. Kwo, C. Majkrzak, R. C. C. Ward, and A. Schreyer, *Phys. Rev. B* **82**, 014426 (2010).
- [13] S. V. Grigoriev, D. Lott, Yu. O. Chetverikov, A. T. D. Grünwald, R. C. C. Ward, and A. Schreyer, *Phys. Rev. B* **82**, 195432 (2010).
- [14] V. V. Tarnavich, D. Lott, S. Mattauch, A. Oleshkevych, V. Kapaklis, and S. V. Grigoriev, *Phys. Rev. B* **89**, 054406 (2014).
- [15] V. V. Tarnavich, A. S. Volegov, D. Lott, S. Mattauch, A. A. Vorobiev, A. Oleshkevych, and S. V. Grigorieva, *J. Surf. Invest.: X-ray, Synchrotron and Neutron Tech.* **8**, 976 (2014).
- [16] V. I. Zverev, A. M. Tishin, Z. Min, Ya. Mudryk, K. A. Gschneidner Jr., and V. K. Pecharsky, *J. Phys.: Condens. Matter* **27**, 146002 (2015).
- [17] S. A. Nikitin, *Magnetic Properties of Rare-Earth Metals* (Mosk. Gos. Univ., Moscow, 1989).
- [18] B. J. Kirby, J. E. Davies, K. Liu, S. M. Watson, G. T. Zimanyi, R. D. Shull, P. A. Kienzle, and J. A. Borchers, *Phys. Rev. B* **81**, 100405(R) (2010).
- [19] J. Jensen and A. R. Mackintosh, *Rare Earth Magnetism: Structures and Excitations* (Clarendon Press, Oxford, 1991).
- [20] K. P. Belov, R. Z. Levitin, and Nikitin S.A., *Sov. Phys. Usp.* **7**, 179 (1964).
- [21] E. V. Tartakovskaya, *JMMM* **381**, 267 (2015).
- [22] Y. Togawa, T. Koyama, K. Takayanagi, S. Mori, Y. Kousaka, J. Akimitsu, S. Nishihara, K. Inoue, A. S. Ovchinnikov, and J. Kishine, *Phys. Rev. Lett.* **108**, 107202 (2012).
- [23] A. Gibaud, D. F. McMorrow, and P. P. Swaddling, *J. Phys.: Condens. Matter* **7**, 2645 (1995).
- [24] V. O. Golub, V. V. Dzyublyuk, A. I. Tovstolytkin, S. K. Arora, R. Ramos, R. G. S. Sofin, and I. V. Shvets, *J. Appl. Phys.* **107**, 09B108 (2010).